Original Article

Thermal and mechanical properties of PLA-based multiscale cellulosic biocomposites

M.A. Ruz-Cruz [a], P.J. Herrera-Franco [a], E.A. Flores-Johnson [b],
M.V. Moreno-Chulim [a], L.M. Galera-Manzano [a], A. Valadez-González [a,*]

[a] Centro de Investigación Científica de Yucatán, A.C., Unidad de Materiales, Calle 43 # 130 Entre 32 y 34, Col. Chuburná de Hidalgo, C.P. 97205, Mérida, Yucatán, Mexico
[b] CONACYT-Unidad de Materiales, Centro de Investigación Científica de Yucatán, A.C., Unidad de Materiales, Calle 43 # 130 entre 32 y 34, Col. Chuburná de Hidalgo, C.P. 97205, Mérida, Yucatán, México

ARTICLE INFO

ABSTRACT

In this work polylactic acid (PLA) based multiscale cellulosic biocomposites were prepared with the aim to evaluate the effect of the incorporation of cellulose nanocrystals (CNCs) on the PLA biocomposites reinforced with cellulose microfibers (MFCs). For this, PLA composite materials reinforced with both MFCs and with a combination of MFCs and CNCs were prepared, while keeping the content of cellulosic reinforcements constant. The thermal and mechanical properties of these multiscale PLA biocomposites were characterized by thermogravimetry (TGA), differential scanning calorimetry (DSC), flexural mechanical and, dynamic mechanical (DMA) tests. Likewise, they were characterized by Fourier transform infrared spectroscopy (FTIR) and scanning electron microscopy (SEM). The results show that the replacement of MFCs by CNCs in the 1–5% range appreciably modifies the thermal and mechanical properties of multiscale compounds. For example, they increase the thermal stability of the materials, modify the PLA crystallization process and play the role of adhesion promoters since the mechanical properties in flexure increase in the order of 40% and the storage modulus increases in the order of 35% at room temperature. Also, the addition of CNCs increases the relaxation temperature of the material from 50 to 60 °C, thereby expanding the temperature range for its use.

1. Introduction

Polylactic acid (PLA) is a versatile biopolymer made from the polymerization of lactic acid obtained from the fermentation of renewable agricultural raw materials. It belongs to the family of aliphatic polyesters. It has attracted attention because of its biodegradability, biocompatibility, transparency, high elastic modulus and, strength. Moreover, its processing is similar to that used for polyolefins or other thermoplastics [1–3]. However, its limited melt strength, low heat distortion temperature, high brittleness, and low flexibility limit its use. One strategy to improve the properties of PLA is the addition of natural fibers such as cellulosic fibers

[4—6] as reinforcements. Cellulose is the main component of the plant cell wall and shows excellent mechanical and thermal properties besides being biodegradable [7—9].

Due to the rise of nanotechnology, the production of nanosized cellulose fibers has attracted many researchers [1,10—14]. Nano cellulose is a material that is isolated from cellulose where at least one of its dimensions is in the nanoscale (<100 nm). Generally, there are three types of nano cellulose, including cellulose nanofibrils (CNF), cellulose nanocrystals (CNC), and bacterial nano cellulose (BNC) [10]. Due to the reduction of its size, nano cellulose has a higher surface area, crystallinity, better optical transparency, and enhanced mechanical, thermal, and barrier properties. Additionally, nano cellulose is renewable, biodegradable, biocompatible, and nontoxic [11]. These beneficial properties make nano cellulose a promising resource for reinforcement in polymer nanocomposite. Also, their surface hydroxyl groups provide the opportunity for surface modification to improve their compatibility with polymer matrices and to impart special functionalities for their use in biomedical, water treatment, electronics, energy fields, and other applications [12—14]. However, these nanomaterials also possess some disadvantages, including high moisture absorption and strong incompatibility with hydrophobic polymeric matrices such as polyolefins and PLA. Chakrabarty and Teramoto [12] pointed out the need to introduce either covalent or non-covalent chemical interactions between the polymer and the nanocellulose to achieve the desired performance and functionalities. They emphasized that the type and extent of the physical and chemical interactions are the main factors that govern the dispersibility of nanocellulose in the polymeric matrix and, therefore, the final properties of the nanocomposite. CNCs are produced by acid hydrolysis, which disintegrates amorphous domains, that is, the longitudinal sections of the microfibrils. Their average length is generally of the order of a few hundred nanometers, and the width is of the order of a few nanometers [10]. The incorporation of these materials in non-polar thermoplastic matrices such as polyolefins or low polar ones such as PLA leads to agglomeration problems and limits their content to low concentrations. Graupner and Müssig [8] compared differences between thermoplastics reinforced with cellulose microfiber (MFC) at 30wt.% of fibers with PLA or polypropylene (PP) matrix, observing increases in tensile strength, Young's modulus, and hardness; these values are significantly higher for PLA and its compounds compared to PP. However, PLA is brittle while PP shows ductile stress—strain behavior. The impact strength of PLA increased by adding lyocell while the impact resistance of PP decreased. Other authors [15,16] made poly (lactic acid) (PLA) composites and cellulosic fibers by combining the wet-laid fiber sheet forming method with the film stacking composites manufacturing process. The addition of pulp fibers increased the storage modulus and the elasticity; promoted cold crystallization and recrystallization of PLA as well as a dramatic enhancement of the composite's elastic modulus and strength. On the other hand, the development of nanofiber-reinforced composites has experienced great growth in recent years. Siqueira et al. [14] presented in a review, different processing alternatives to improve the distribution of nanocellulose since they have the disadvantage of

low dispersion in nonpolar matrices. Siró and Plackett [17] carried out various chemical and/or enzymatic treatments to overcome the dispersion problem of fiber reinforcements and the formation of a better interface, a challenge associated with the use of nano cellulose. Eichhorn et al. [18], reviewed the processing and characterization of cellulosic nanofibers, divided them by the type of source material, the volumes of nano cellulose, and the analysis of the interfacial properties of the nanocomposites. Dzul-Cervantes et al. [19], grafted maleic anhydride (MA) onto PLA and used this PLA-g-MA as a coupling agent in the production of PLA/cellulose composites to improve the fiber-matrix compatibility. For their part, Oksman et al. [20], report that the use of maleated-PLA (PLA-g-MA) as a coupling agent increases the tensile mechanical properties of PLA/nano cellulose biocomposites.

Several studies have recently been reported that include the incorporation of reinforcements whose dimensions vary by at least one order of magnitude. These materials, called hierarchical or multiscale, have been developed with the idea of establishing a synergy between the fibrous reinforcements and the polymeric matrix, mainly thermoset (epoxy) matrices [21—23] and some thermoplastics such as PLA [4,24,25]. Okubo et al. [24], developed a two-stage process for the production of new multiscale biocomposites based on a PLA reinforced with micro-fibrillated cellulose and bamboo fiber bundles. First, they premixed the micro-fibrillated cellulose and PLA using a roller mixer, followed by drying and grinding. This blend was injected into a mold that already contained the arrangement of bamboo bundle fibers. They found that by adding only 1wt. % of micro-fibrillated cellulose, an increase in fracture energy of almost 200% was obtained because the cellulose acts as reinforcement that prevents sudden interface crack growth. Also, the authors report that cellulose tends to accommodate in the interfacial region between the PLA and the bamboo fibers because of its relative scale difference with bamboo. Blaker et al. [26], produced unidirectional laminates of long fibers of PLA, covered with BNC grown in situ, comparing them with laminates containing functionalized nanocellulose in the PLA matrix, they studied the mechanical properties under quasi-static conditions and reported that the orientation of the chain induced by deformation due to melt spinning enhance nucleation and crystal growth and increase PLA tensile modulus and resistance.

This structural hierarchy can play an important role in determining material properties. While the main reinforcements promote improvements in mechanical properties, the addition of nano-reinforcements contributes to improvements in the increase in energy absorption to reach fracture and changes in the crystallization of the material. Understanding the effects of the hierarchical structure can guide the synthesis of new materials with physical properties adapted to specific applications [27]. However, the studies made so far are incipient. These composite materials have the characteristic that the longer fibers are the main reinforcement, while the nanometric fibers create bridges with the matrix to prevent sudden crack growth [24,27]. The objective of the work presented in this paper is to evaluate the effect of incorporating CNCs on PLA/MFC and using PLA-g-MA as a coupling agent, in cellulose-reinforced PLA-matrix multiscale biocomposites.

2. Experimental

2.1. Materials

PLA 3251D from NatureWorks®, having a number average molecular weight (Mn) of 32.2 kg/mol, a glass transition temperature at 55 °C, and a melting point of 160 °C was used as a matrix. Cellulose microfibers (MFC) having 500 ± 35 μm in length and 12 ± 2 μm in diameter were obtained from henequen fibers (*agave fourcroydes*) according to the methodology described by Dzul-Cervantes et al. [19]. Cellulose nanocrystals (CNCs) were purchased from the University of Maine Process Development Center. Their properties are listed in Table 1.

The PLA-g-MA used as a coupling agent was prepared according to the methodology reported in [19].

2.2. Composite preparation

The multiscale bio composites described in Table 3 were fabricated using a BRABENDER mixing chamber with three heating zones. A temperature of 170 °C was set in all three zones . The rotation speed of the blades was 50 rpm and a mixing time of 20 min was used. Different combinations of mixing time, blade speed, temperatures of the heating zones, and drying time of the materials were carried out to establish the aforementioned mixing procedure. The change in the molecular weight, using an Agilent 1100 GPC, and the change in the glass transition temperature (Tg) and the melting temperature (Tm), using Differential Scanning Calorimetry (DSC), were used to monitor the degradation of the PLA due to the processing. Table 2 shows the results corresponding to the PLA matrix before and after being processed.

As can be seen in these results, the degradation of PLA is less than 5%.

The composites were molded using a compression molding press. The press temperature was 170 °C and the pressure was 5500 lb. Specimens were cut from a lamina according to the ASTM D790 standard [29]. The specimens were stored in glass desiccators at a constant temperature of 25 ± 1 °C and relative humidity of 50 ± 2% until testing.

2.3. Analytical characterization

2.3.1. Photoacoustic fourier transform infrared spectroscopy (FTIR-PAS)

Interferometer-based FTIR photoacoustic spectroscopy (FTIR-PAS) is a surface technique that allows distinguishing the bulk of the sample from its surface because the signal is generated from a few micrometers of the surface and provides

Table 1 – Properties of CNCs.

CNC[a]	Dimensions (nm)		Surface energy (mJ/m^2)		
	Length	Width	γ^d	γ^p	γ
	296 ± 10	21 ± 2	39	15	54

[a] Moo-Tun et al. [28].

Table 2 – PLA properties before and after processing.

PLA	GPC	DSC	
	Mn (Kg/mol)	Tg (°C)	Tm (°C)
As received pellet	32.4	59	170
Processed	27.6	59	169

Table 3 – Composition of Multiscale biocomposites studied.

Nomenclature	PLA(%)	MFC (%)	CNC (%)
PLA	100	0	0
PLA/MFC	80	20	0
PLA/MFC/CNC1	80	19	1
PLA/MFC/CNC5	80	15	5

information about the chemical structure of the near-surface region. The main advantage of photoacoustic spectroscopy is that no elaborate sample preparation is required. This technique is non-destructive and can be used to analyze materials that are difficult to homogenize or the structure or the chemical composition change during grinding. Even samples with rough surfaces and strongly scattering infrared light can be easily measured since the photoacoustic signal is proportional to the absorbed energy, not reflected as reflectance techniques [30–32]. Essentially, the method is based on generating acoustic waves by illuminating a sample with modulated light. Absorption of this modulated radiation, followed by non-emissive decay, causes the generation of modulated heat. It gives rise to periodic temperature oscillations within the sample, which produce pressure oscillations to the sample's gas. A microphone detects these pressure oscillations as an acoustic wave converted into an electrical signal and then into the corresponding spectrum.

The biocomposites samples were dried in a vacuum oven at 60 °C for 24 h and then analyzed in a Thermo Scientific Nicolet 8700 model spectrophotometer. The samples were analyzed using the photoacoustic PAC 300 detector accessory (MTEC Photoacoustics Inc., USA) with 60 scans and a resolution of 8 cm^{-1}. The cell compartment was purged with helium for 5–10 s; next, the helium flow was stopped, and the spectrum was measured. Before each FTIR-PAS measurement, the background was recorded using highly pure compressed graphite (carbon black) as a standard reference sample.

2.3.2. Thermogravimetric analysis

The thermal behavior analysis of each material (10 mg) was carried out in a TGA 7 PerkinElmer Thermogravimetric Analyzer in the temperature range of 40–600 °C, at a heating rate of 10 °C/min, in a nitrogen environment. The thermograms were recorded by triplicate and the results reported are the average of the three measurements.

2.3.3. Differential scanning calorimetry analysis

Differential Scanning Calorimetry (DSC) analyzes were performed with a PerkinElmer DSC7 Differential Scanning Calorimeter. Each sample weighing 5–10 mg was sealed in an aluminum tray and heated under nitrogen flow at heating rate of 5 °C/min, and kept at this temperature for 1 min to erase

thermal history, subsequently; the sample was cooled and reheated under the same conditions. The analysis was performed twice and the average results were reported.

The glass transition (Tg), the cold crystallization (Tcc), the melting temperatures (Tm), as well as the enthalpies of melting and cold crystallization of the samples were determined from the second heating series. The percentage of crystallinity of the cold melting and crystallization stages, as well as the global crystallinity of the biocomposites, were calculated with the following formulas:

$$X_m = \frac{\Delta H_m}{(w_{PLA} \Delta H^0_m)} 100 \qquad (1)$$

$$X_{cc} = \frac{\Delta H_{cc}}{(w_{PLA} \Delta H^0_m)} 100 \qquad (2)$$

where:

X_m is the melting crystallinity, X_{cc} is the cold crystallinity, ΔH_m and ΔH_{cc} are the enthalpies of fusion and crystallization respectively (J/g), ΔH^0_m is the 100% crystalline PLA's fusion enthalpy taken as 93 J/g [33] and W_{PLA} is the weight fraction of the PLA phase in the composite.

2.3.4. Flexural mechanical analysis

The mechanical properties of the composites were measured using a Shimadzu model AGS universal testing machine with a head speed of 0.3 mm/min and a 1 kN load cell. The bending test was carried out following the D790 standard [29], for bending tests on composites and plastics. At least five samples were analyzed for each composite material, and the results are presented as an average for the samples analyzed.

2.3.5. Dynamic-mechanical analysis

The dynamic-mechanical flexural tests as a function of temperature were carried out in a DMA 7 PerkinElmer with a temperature sweep from 0 to 170 °C, with a heating ramp of 5 °C per minute and a frequency of 1 Hz per second.

2.3.6. Morphological analysis

The multiscale bio composites' fracture surfaces were characterized using a JEOL SEM model JSM-6360 LV scanning electron microscope operated at 20 kV. The samples were covered with gold.

3. Results and discussions

3.1. Photoacoustic fourier transform infrared spectroscopy (FTIR-PAS)

The FTIR spectra of PLA, PLA/MFC, PLA/MFC/CNC1, and PLA/MFC/CNC5 are shown in Fig. 1. The PLA characteristic peaks can be observed in Fig. 1(a). The one corresponding to the vibration of the asymmetric stretching of the C−H bond at 2988 cm^{-1}, a strong absorption peak characteristic at 1750 cm^{-1} and 875 cm^{-1} owing to stretching vibrations of C=O and C−COO bonds, respectively [25,31] and the stretching vibration peaks of C−O−C and C−C at 1190 cm^{-1} and 1130 cm^{-1} respectively [28,34].
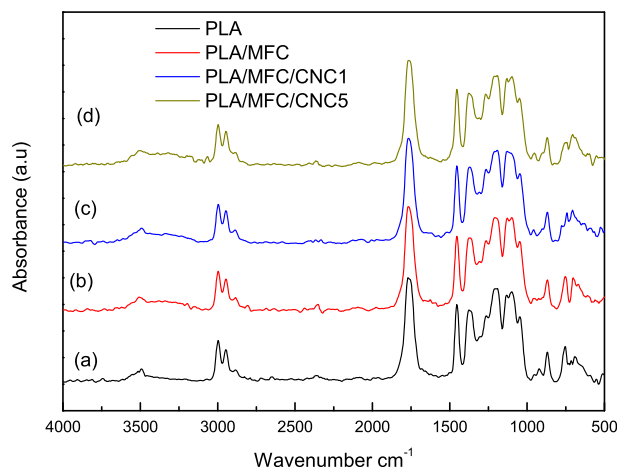
Fig. 1 − FTIR spectra for: a) PLA, b) PLA/MFC, c) PLA/MFC/CNC1, d) PLA/MFC/CNC5 biocomposites.

In Fig. 1(b) the PLA/MFC, bands between 3500 and 3300 cm^{-1} and from 3000 to 2850 cm^{-1} are observed that are attributed to the stretching group of the −OH and −CH groups, respectively, characteristic of cellulose [28,34−36], the characteristic PLA peaks described above can also been observed. Also, some new peaks at 2888 cm^{-1} and 1600 cm^{-1} that can be attributed to the presence of the anhydride maleic used as a coupling agent can be appreciated in Fig. 1(b). Regarding Fig. 1(c) and (d), it can be seen that both spectra are similar to that of 1(b). This result is expected since the characteristic bands of the CNCs are essentially the same as those of cellulose microfibers [37]. Galera-Manzano et al. [25], in a study related to the biodegradation of similar multiscale biocomposites, report that before their biodegradation, their FTIR spectra are very similar and as the biodeterioration of the materials occurs that changes in the spectra are observed, mainly due to a change in the composition on the surface of the material.

3.2. Thermal analysis

3.2.1. Thermogravimetric analysis

The thermograms of the mass loss for the PLA, PLA/MFC, PLA/MFC/CNC1, and PLA/MFC/CNC5 are presented in Fig. 2(a) while their respective derivatives of the mass losses are presented in Fig. 2(b). The summary of the percentages of degradation concerning temperature are presented in Table 4, where some temperatures occur at different percentages of degradation (10, 25, and 50%) of weight loss; Tr is the temperature where the percentage of mass loss becomes constant; Tder is the temperature of higher degradation rate and %$_{Resid}$ is the percentage of carbon residues for the materials at the end of the test.

Fig. 2(a) shows that PLA degradation occurs in a single stage, no mass losses are observed up until 220 °C approximately, continuing with similar trends up to 270 °C, with a loss of mass of 3%. At 332 °C, the percentage of carbon residues is equal to 0%, so there is a 100% degradation. It can also be seen In Fig. 2(b) how the degradation occurs in a single step, with a maximum degradation temperature of 316 °C for PLA. Similar results were reported by Abubakar et al. [34] and Johari et al. [35].
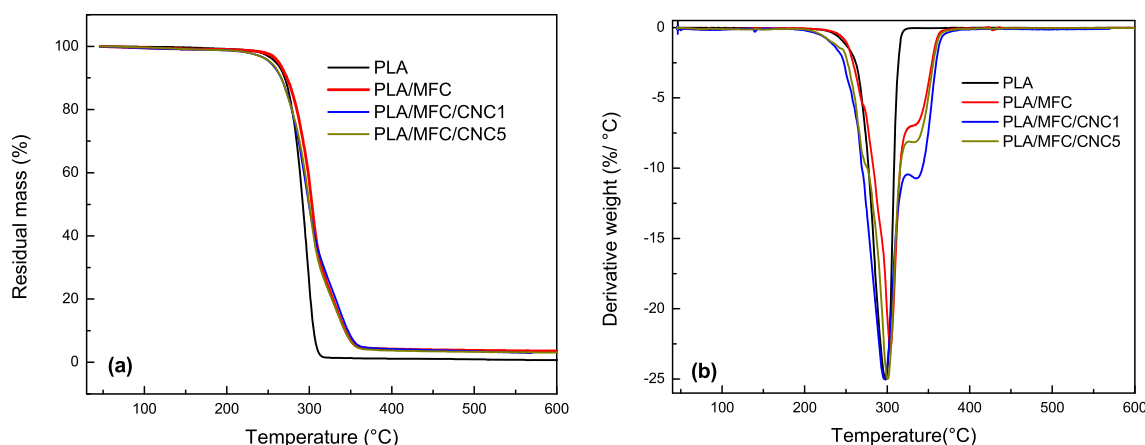
Fig. 2 – (a) Residual mass thermograms and (b) their derivatives, for the studied biocomposites.

Table 4 – Temperature values for different degradation percentages for the different materials.

Material	Loss mass (%)			T_r (°C)	T_{der} (°C)	% Resid.
	T_{10} (°C)	T_{25} (°C)	T_{50} (°C)			
PLA	270 ± 2	292 ± 1	303 ± 3	329 ± 1	316 ± 2	0
PLA/MFC	290 ± 2	307 ± 2	314 ± 4	360 ± 2	316 ± 2	3.5 ± 0.2
PLA/MFC/CNC1 AM 19MFC	265 ± 3	284 ± 3	298 ± 2	360 ± 2	296 ± 3	3.5 ± 0.1
PLA/MFC/CNC5	265 ± 2	284 ± 3	298 ± 3	360 ± 1	300.7 ± 2	3.5 ± 0.2

The weight loss for PLA/MFC from 50 °C to 150 °C, which can be attributed to evaporation of moisture can be seen in Fig. 2(a). Weight loss between 150 and 250 °C is indicative of depolymerization of non-cellulosic structures such as hemicellulose (breaking of glycoside bonds) and water adsorbed by the fibers. At temperatures between 300 and 350 °C, the degradation of α-celluloses occurs, absorbing a large amount of energy. This reveals that the amorphous structure and the crystallinity of cellulose are related to the degradation of the sample; it also indicates that the crystalline sample has high thermal stability. The degradation stages for PLA/MFC correspond to the evaporation and removal of adsorbed water, the breaking of the glycosidic bonds of cellulose, leading to H_2O and CO_2, alkanes, and other derivative hydrocarbons which occurs at temperatures between 230 and 370 °C. After 380 °C, the decomposition products have a low degradation [38]. These stages can be observed in the curves of the derivative of mass loss for PLA/MFC (Fig. 2(b)), where a weight loss is observed at the beginning due to water and then at 250 °C the degradation of hemicelluloses and α-cellulose is observed. On the other hand, the weight loss curve is not constant because at the test temperatures, the degradation of the cellulose constituent materials was not achieved; in addition, this ash formation is related to the hemicellulose content in the material. The trend in mass losses continues similarly for the two materials up to 240 °C, at 330 °C occurs cellulose degradation. After 370 °C, there are no more losses and the carbon residue is 3.5%, due to the presence of cellulose.

In Fig. 2(b) the derivatives of the weight loss for the temperature for the composite materials are shown, where it can be observed that the degradation is in two stages, the

first one can be assigned to the degradation of the matrix, and the second degradation drop corresponds to the cellulosic fibers.

The mass loss curves concerning the temperature of biocomposites which contain 1 and 5% of cellulose nanocrystals conserve 20% by weight of reinforcements of the material, considering that at this concentration the highest improvements in properties have been reported [39]. As can be seen, the weight loss of the materials begins before 100 °C, which could be due to the evaporation of surface water from the composite materials, with materials containing reinforcements having a greater slope, which suggests that cellulose absorbs more water. The weight loss that continues after 100 °C to approximately 150 °C could correspond to the water adsorbed by the fiber during its processing and therefore can only be released when there is greater mobility in the chains of the composite material. For PLA without fiber changes are not observed in this temperature range [35]. After 150 °C, the mass loss is very similar for all materials up to approximately 200 °C where it is observed that there is a change in the degradation behavior since the materials that have CNCs begin to have greater weight loss, this suggests that the CNCs (which increase the viscosity during processing) could affect and further decrease the size of the PLA chains [28,34,35], which can also be observed in the curves of the derivative of loss of mass.

The curves of the derivatives for the materials with and without CNCs are shown in Fig. 2(b). It can be observed that the degradation occurs in two stages for the materials with reinforcements, the first for the degradation of PLA and some volatiles of MFC and CNCs and the second for crystalline

celluloses, the trend show differences in the degradation rate for materials that have CNCs with those that do not. It can also be observed that the temperature at which degradation begins is higher for materials that do not contain CNCs, occurring in a range between 296 and 303 °C. The average temperatures for different percentages of loss of mass of the composite materials are shown in Table 4. The incorporation of MFC increases the thermal stability of the material, however, the addition of CNCs did not generate a significant change and even decreased the temperature when there was a degradation of 10%. An improvement is only seen after a loss of 25% with an increase in temperature and becomes significant in Tr where differences of more than 45 °C were observed, which can be attributed to the presence of coupling agent. Furthermore, it is also observed that the formation of residues is generated with the incorporation of the fiber, which suggests a fire-retardant effect in the matrix [35].

3.2.2.   Calorimetric analysis

The curves of the second heating were analyzed for the evaluation of the thermal properties of the materials. Fig. 3 shows the thermograms obtained for PLA, PLA/MFC, PLA/MFC/CNC1, and PLA/MFC/CNC5 respectively. In these, it can be seen that all the materials show three characteristic transitions of PLA, glass transition, cold crystallization, and fusion [40]; their corresponding data are represented in Table 5.

The glass transition temperature (Tg) is a complex phenomenon that is based on several factors, such as intermolecular interaction, the flexibility of the chain, and the molecular weight of the material. The exothermic peaks that represent the cold crystallization (Tcc), obtained during the second heating cycle, are attributed to the reorganization of the amorphous domains in crystalline regions because of an increase in macromolecular flexibility and mobility of the chain with increasing temperature [35]. Furthermore, when comparing the Tcc for materials with and without re-inforcements, a shift to the left can be observed which suggests that cellulosic fibers act as nucleating agents and therefore crystallization occurs at lower temperatures [1]. The
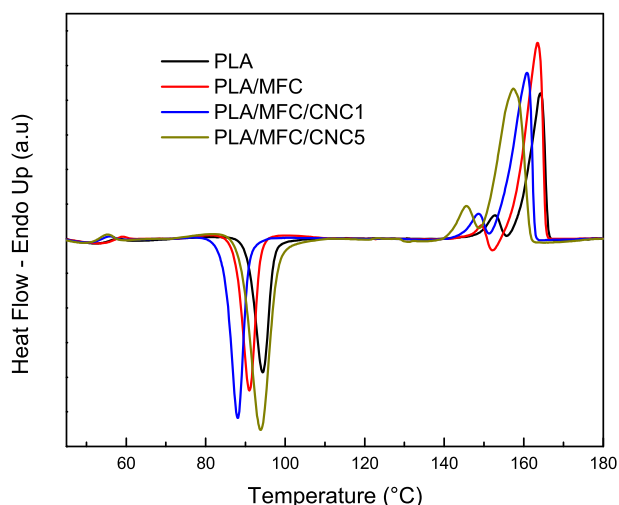
T_{CC} value of the composite materials decreased for those containing fibers concerning PLA which could be due to the effect of nucleation of the fibers on the crystallization of the composite material [40,41]. It was observed that the melting transition (T_m) for all materials has a double peak, T_{m1}, and T_{m2}. This behavior is probably due to the loss of chain alignment and the conformational purity of the PLA matrix during the mixing process. In fusion, in addition, the shoulder peak at a lower temperature T_{m1} is assigned for a less perfect or disordered crystalline structure or a decrease in the size of the crystallites, so it could be assigned as an α' transition. Regarding the materials crystallinity, X_m, it was very similar and it is known that this depends, in addition to the nucleating agents, the size of the polymer chains, the heating rate, in such a way that the lower Whatever this ramp, this allows more time for the positioning of chains [41].

In Fig. 3, the typical curves of heat absorption concerning the temperature for the composite materials with different concentrations of CNCs are shown. In Table 5, the thermal characteristics obtained for the different composite materials are shown.

In Table 5, we can see that the Tg value is slightly higher for the material that does not have CNCs. It is believed that CNCs can act as an insert between the chains, favoring their mobility [2].

It can be observed in Table 5 that Tcc decreases when the concentration of the CNCs increases, which may be indicative of the nucleation effect of the CNCs [2,42]. Also, the values of T_{m2} are similar for the materials of PLA 20 MFC and PLA 19 MFC, which contain 1% of CNCs. Perhaps due to the low concentration of CNCs, no significant effect is observed. For those containing 5% CNCs, the shift to the left is more significant, indicating that CNCs favors nucleation and crystal growth on their surface [2].

It is interesting to note that the inclusion of the cellulosic fibers promotes a cold crystallization, and the melting crystallinity of the composite is lower than that of PLA. This could be attributed to better adhesion between the cellulosic fibers and the matrix due to the PLA-g-MA coupling agent used. In the case of the multiscale biocomposites, it can be seen that the inclusion of the CNCs decreases both the cold and the melting crystallinity, compared to PLA/MFC composites. The decrement goes from 37% to 33% and 26% when the NCC content increases from 1% to 5% respectively. This interesting result suggests that CNCs either improve the adhesion between cellulosic fibers and the PLA matrix by acting as adhesion promoters or perhaps their presence interferes with the growth of crystals nucleated by cellulosic fibers [35,42]. More studies are needed to elucidate the role that CNCs play in the crystallization of PLA in this type of composite material.

3.3.   Mechanical characterization

3.3.1.   Flexural test

The flexural mechanical properties are shown in Fig. 4. An improvement in the flexural strength (FS) of all composite materials is observed in Fig. 4(a). Adding a 20% w/w of cellulose fibers increases the PLA FS by approximately 80%. When 1% of the cellulosic fibers are replaced by 1% CNCs the FS of

Fig. 3 − DSC Thermograms for the studied biocomposites.

Table 5 — Second heating results for multiscale biocomposites studied.

Material	T_g (°C)	T_{cc} (°C)	T_{m1} (°C)	T_{m2} (°C)	X_{cc} (%)	X_m (%)
PLA	53 ± 1	94 ± 2	151 ± 1	162 ± 2	32.7 ± 1.5	40.3 ± 0.5
PLA/MFC	55 ± 2	90 ± 3	149 ± 2	161 ± 1	33.3 ± 1	37.8 ± 1
PLA/MFC/CNC1	53 ± 2	88 ± 3	149 ± 1	161 ± 3	23.4 ± 2	33.3 ± 0.8
PLA/MFC/CNC5	52 ± 1	86 ± 2	146 ± 3	157 ± 2	24.0 ± 1	26.8 ± 1
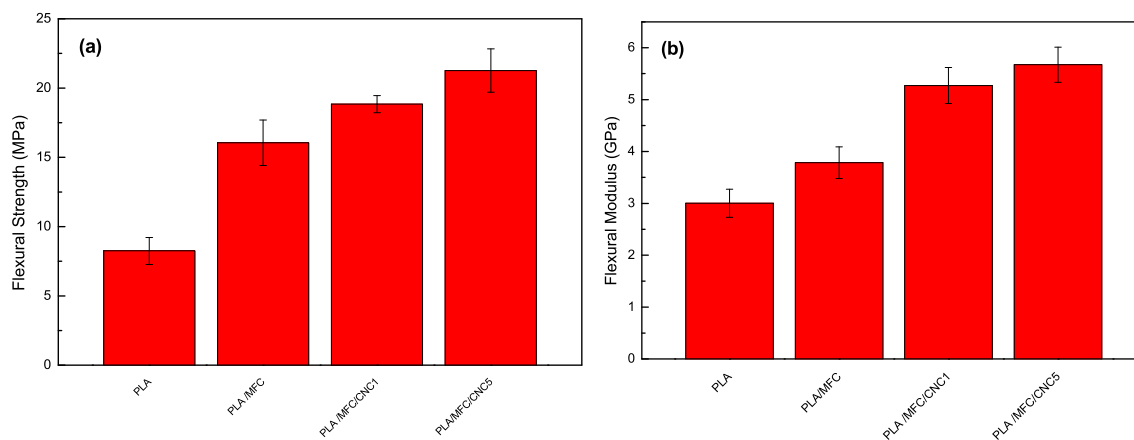
Fig. 4 — (a) Flexural Strength and (b) Modulus of the studied biocomposites.

the biocomposite increases 130% compared to PLA. Moreover, replacing 5% of MFC by CNCs increases the FS of the multiscale biocomposite around 175%. This behavior suggests a more efficient stress transfer at the fiber-matrix interphase [43]. The stress transfer efficiency cannot be attributed to the role of the PLA-g-MA coupling agent but to the presence of the CNCs that could be reinforcing the interphase region between the MFC and the PLA, (see schemes 1 and 2 in supplemental data).

Also, this improvement could be attributed to the formation of entanglement between the cellulose nanocrystals and the cellulose microfibers in the composite material, which could delay fracture [44,45]. It will be necessary to perform additional studies to elucidate these improvements.

Fig. 4(b) shows the flexural modulus of PLA and the biocomposites. The flexural modulus of PLA is 3 GPa and the modulus of PLA/MFC increases approximately 25%. However, the elastic modulus of PLA/MFC/CNC1 and PLA/MFC/CNC5 is 67% and 82% higher, both compared with the pristine PLA. This improvement, again, is attributed to the fact that CNCs are acting as a PLA-MFC interphase reinforcement [45].

3.3.2. Dynamical characterization

Dynamic mechanical analysis (DMA) determines the storage modulus (E′) and the damping coefficient (Tan δ) as a function of temperature. DMA identifies the transition regions in polymers and allows knowing the operating temperatures of the materials [46]. In Fig. 5(a), it can be seen that the inclusion of the MFC increases the storage modulus and raises the thermal stability of the biocomposites. These improvements

may be attributed to the anchoring of the fibers in the matrix, causing more energy to be required to move the polymer chains and to a better dispersion of the MFC, resulting in a more effective stress transfer between matrix and the cellulose reinforcements [41,47]. An additional increment in the storage modulus and thermal stability is noticed when CNCs are added. The increase of storage modulus for the biocomposite material with 5% CNCs is higher but, there is no evident increment in the thermal stability compared with the 1% CNCs.

Fig. 5(b) shows plots of tan δ vs temperature. The increase in the relaxation temperature α in the materials can be seen, and in this case, it refers to their Tg. A larger area under the α relaxation peak in the tan δ curves of a polymer indicates that the molecular chains exhibit a higher degree of mobility, hence better damping properties [48]. For materials that do not have the reinforcements, relaxation begins at 50 °C, with a peak at 59 °C, with areas of curves much smaller than those of other reinforced materials, which indicates that the fibers are interacting with the matrix and higher temperature is required to achieve movement of the polymer chains.

For hierarchically reinforced materials, the transition temperatures observed are 62 and 64 °C, when they contain 1% and 5% of CNCs. It may be attributed to the higher number of bonds formed between the CNCs and the matrix. Also, the curve for materials with 5% CNCs has almost no area under the curve, while for 1% the area is very visible, which could be because, as the area of the curve is proportional to the number of chains that participate in the relaxation, which infers good
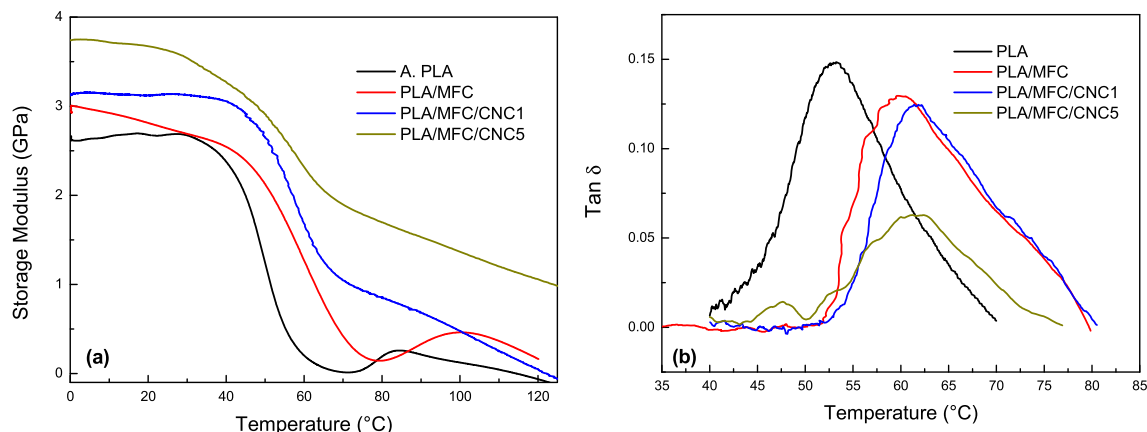
Fig. 5 – Dynamical mechanical properties of studied biocomposites at 5 °C/min (a) Storage Modulus and (b) Tan δ

compatibilization between the reinforcements and the matrix. This decreases due to possible fiber agglomeration because of the high content of CNCs, causing that the chains that participate in the relaxation are much less [2].

Fig. 6 shows the behavior of the multiscale materials studied with a temperature ramp of 3 °C/min, which is a rate frequently used in the works reported in the literature. A change in the behavior of PLA can be observed at temperatures both below and above the Tg. Below the Tg, there is a slight increase of the modulus due to the crystallization of the material, but it abruptly falls around the Tg indicating an evident recovery of the storage modulus due to the recrystallization of the material around 90 °C.

The changes are not as evident as with PLA because the presence of cellulosic fibers restricts the movement capacity of the molecular chains of PLA. However, replacing MFC for 1% and 5% of CNCs makes the composite material much more robust since its behavior is very similar to that observed with the heating rate of 5 °C/min, (see in Fig. 6(b)). These results suggest there is a synergy between the cellulosic reinforcements, perhaps due to the ability of the CNCs to act as reinforcing elements of the PLA-MFC interphase.

3.3.3. Morphological analysis

Fig. 7 shows the SEM micrographs for MFC, composites with 20% MFC, and MFC composites with 1 and 5% CNCs, (a total percentage of reinforcement of 20% is kept). Fig. 7(a) shows the surface fracture micrograph for PLA/MFC. Good adhesion between the cellulose fibers and the matrix is observed, due to the presence of a PLA-g-MA coupling agent [40,41]. It is seen that the distribution of the reinforcements is more uniform since clean areas without fibers are not observed; also, there are fewer agglomerations between the fibers, since the filaments are observed. As in the micrographs of the material without a coupling agent, it is observed that the fibers do not present damage, and the gaps where the fibers debonded from the matrix are present. Furthermore, in this case, there are traces of the matrix adhered to the fibers, indicating that the failure was in the matrix [24].

Fig. 7(b) and (c), shown the fractures of the composite materials with 20% of reinforcements, but with 1 and 5% of CNCs, respectively, in this material, characteristics similar to the materials with coupling agent are observed, that is, better dispersion and the presence of matrix residues on the MFCs.

Fig. 6 – (a) Storage Modulus of studied biocomposites at 3 °C/min scan rate and (b) Multiscale biocomposites comparison.
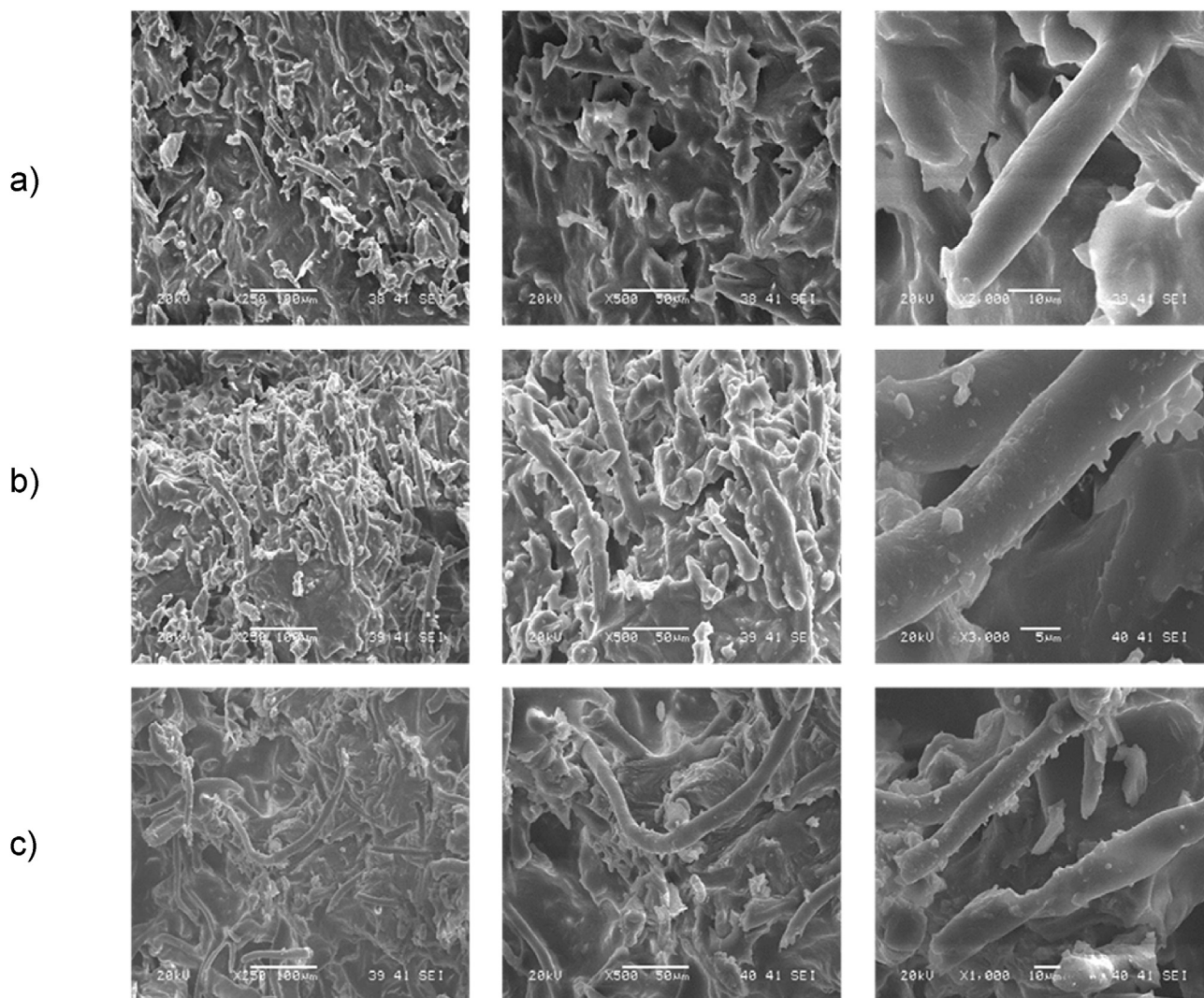
Fig. 7 — SEM micrographs of composite materials a) PLA/MFC, b) PLA/MFC/CNC1, c) PLA/MFC/CNC5.

4.   Conclusions

PLA-based multiscale cellulosic biocomposites were prepared with the aim to evaluate the effect of the incorporation of cellulose nanocrystals on the thermal and mechanical properties of PLA reinforced with cellulose microfibers. For this, PLA composite materials reinforced with cellulose microfibers (MFC) and reinforced with a combination of micro and nano cellulose fibers were prepared, while keeping the content of cellulosic reinforcements constant. From the results, it is noticed that replacing cellulose microfibers with cellulose nanocrystals in the 1—5% range appreciably modifies the thermal and mechanical properties of multiscale composites. For instance, the fibers appreciably increase the thermal stability of the materials, modify the PLA crystallization process and play the role of adhesion promoters since the mechanical properties in flexure increase in the order of 40% and the storage modulus increases in the order of 35% at room temperature.

The addition of CNCs, for the formation of hierarchical materials, increases the relaxation temperature of the material from 50 °C to 60 °C, thereby expanding the temperature range for its use.

The behavior of the PLA crystallization process was unexpected, the higher the CNCs content, the lower the crystallization of the multiscale biocomposites was. This interesting result suggests that CNCs improve the adhesion between cellulosic fibers and the PLA matrix by acting as adhesion promoters or perhaps their presence interferes with the growth of crystals nucleated by cellulosic fibers. More studies are needed to elucidate the role that CNCs play in the crystallization of PLA in this type of composite material.

Declaration of Competing Interest

The authors declare no conflicts of interest.

Acknowledgments

Appendix A. Supplementary data

Supplementary data to this article can be found online at https://doi.org/10.1016/j.jmrt.2022.02.072.

REFERENCES

[1] Khoo RZ, Ismail H, Chow WS. Thermal and morphological properties of poly (lactic acid)/nanocellulose nanocomposites. Procedia Chem 2016;19:788—94. 2016.

[2] Mathew AJ, Oksman K, Sain M. The effect of morphology and chemical characteristics of cellulose reinforcements on the crystallinity of polylactic acid. J Appl Polym Sci 2006;101:300—10.

[3] Dubois P, Murariu M. PLA composites: from production to properties. Adv Drug Deliv Rev 2016;107:17—46.

[4] Yousefian H, Azous KB, Rodrigue D. New multi-scale hybrid system based on maple wood flour and nano crystalline cellulose: morphological, mechanical and physical study. J Polym Environ 2016;24:48—55.

[5] Oksman K, Skrifvars M, Selin JF. Natural fibres as reinforcement in polylactic acid (PLA) composites. Compos Sci Technol 2003;63:1317—24.

[6] Jaszkiewicz A, Bledzki AK, Scherzer D. Mechanical properties of PLA composites with man-made cellulose and abaca fibres. Composites: Part A 2009;40:404—12.

[7] Yulianto, Normayulisa D, Saima M, Arbiantia R, Suryanegarab L, Hermansyaha H. Effect of cellulose fiber from sorghum bagasse on the mechanical properties and biodegradability of polylactic acid. Energy Reports 2020;6:221—6.

[8] Graupner N, Müssig J. Cellulose fiber-reinforced PLA versus PP. Int J Polym Sci 2017;2017:1—10.

[9] Elanthikkal S, Gopalakrishnapanicker U, Varghese S, Guthrie J. Cellulose microfibres produced from banana plant wastes: isolation and characterization. Carbohydrate Polym 2010;80:852—9.

[10] Lizundia E, Puglia D, Nguyen T-D, Armentano I. Cellulose nanocrystal based multifunctional nanohybrids. Prog Mater Sci 2020;112:100668.

[11] Nechyporchuk O, Belgacem M, Bras J. Production of cellulose nanofibrils: a review of recent advances. Industrial Crops and Products 2016;93:2—25.

[12] Chakrabarty A, Teramoto Y. Recent advances in nanocellulose composites with polymers: a guide for choosing partners and how to incorporate them. Polymers 2018;10:517.

[13] Dufresne A. Cellulose nanomaterial reinforced polymer nanocomposites. Current Opinion in Colloid & Interface Science 2017;2017:1—8.

[14] Siqueira G, Bras J, Dufresne A. Cellulosic bionanocomposites: a review of preparation, properties and applications. Polymers 2010;2:728—65.

[15] Du Y, Wu T, Yan N, Kortschot M-T, Farnood R. Fabrication and characterization of fully biodegradable natural fiber-reinforced poly(lactic acid) composites. Composites Part B 2014;56:717—23.

[16] Awal A, Rana M, Sain M. Thermorheological and mechanical properties of cellulose reinforced PLA bio-composites. Mech Mater 2015;80:87—95.

[17] Siró I, Plackett D. Microfibrillated cellulose and new nanocomposite materials. Cellulose 2010;17:459—94.

[18] Eichhorn SJ, Dufresne A, Aranguren M, Marcovich NM. Review: current international research into cellulose nanofibres and nanocomposites. J Mater Sci 2010;45:1—33.

[19] Dzul-Cervantes M, Herrera-Franco P, Tábi T, Valadez-Gonzalez A. Using factorial design methodology to assess PLA-g-ma and henequen microfibrillated cellulose content on the mechanical properties of poly(lactic acid) composites. Int J Polym Sci 2017;2017:1—14.

[20] Oksman K, Mathew A, Bondeson D, Kvien I. Manufacturing process of cellulose whiskers/polylactic acid nanocomposites. Composites Sci Technol 2006;66:2776—84.

[21] Hajlane A, Kaddamib H, Joffe R. Chemical modification of regenerated cellulose fibres by cellulose nano-crystals: towards hierarchical structure for structural composites reinforcement. Industrial Crops and Products 2017;100:41—50.

[22] Hajlane A, Kaddami H, Joffe R, Wallstro L. Design and characterization of cellulose fibers with hierarchical structure for polymer reinforcement. Cellulose 2013;20:2765—27778.

[23] Wang K, Chen F, Li Z, Fu Q. Control of the hierarchical structure of polymer articles via "structuring" processing. Prog Polymer Sci 2014;39:891—920.

[24] Okubo K, Fujii T, Thostenson ET. Multi-scale hybrid biocomposite: processing and mechanical characterization of bamboo fiber reinforced PLA with microfibrillated cellulose. Composites 2009;40:469—75.

[25] Galera-Manzano LM, Ruz-Cruz MA, Moo-Tun NM, Valadez-González A, Mina-Hernandez JH. Effect of cellulose and cellulose nanocrystal contents on the biodegradation, under composting conditions of hierarchical PLA biocomposites. Polymers 2021;13:1855.

[26] Blaker J, Lee KY, Walters M, Drouet M, Bismarck A. Aligned unidirectional PLA/bacterial cellulose nanocomposite fibre reinforced PDLLA composites. Reactive & Functional Polymers 2014;85:185—92.

[27] Blaker J, Lee K-Y, Bismarck A. Hierarchical composites made entirely from renewable resources. Journal of Biobased Materials and Bioenergy 2011;5:1—16.

[28] Moo-Tun NM, Valadez-Gonzalez A, Uribe-Calderon JA. Thermo-oxidative aging of LDPE/stearoyl chloride-grafted cellulose nanocrystals blown films. J Polym Environ 2019;27:1226—39.

[29] ASTM-D790 standard test methods for flexural properties of unreinforced and reinforced plastics and electrical insulating materials. Baltimore, MD, USA: ASTM International; 2003. p. 146—54. 8.01.

[30] Dittmar R, Palmer R, Carter R. Fourier transform photoacoustic spectroscopy of polymers. Appl Spectroscopy Rev 1994;29:171—231.

[31] Mohamed A, Gordon S, Biresaw G. Poly(lactic acid)/polystyrene bioblends characterized by thermogravimetric analysis, differential scanning calorimetry, and photoacoustic infrared spectroscopy. J Appl Polym Sci 2007;106:1689—96.

[32] Imani M, Dimic-Misic K, Tavakoli M, Rojas O, Gane P. Coupled effects of fibril width, residual and mechanically liberated lignin on the flow, viscoelasticity, and dewatering of cellulosic nanomaterials. Biomacromolecules 2020;21:4123—34.

[33] Kalita N, Nagarb M, Mudenura C, Kalamdhadc A, Katiyara V. Biodegradation of modified Poly(lactic acid) based

biocomposite films under thermophilic composting conditions. Polymer Testing 2019;76:522—36.

[34] Abubakar I, Azowa N, Umar BY, Zainuddin N, Abdan K, Then Y, et al. Effect of maleic anhydride-modified poly(lactic acid) on the properties of its hybrid fiber biocomposites. Polymers 2017;9:65.

[35] Johari A, Mohanty S, Surendra K, Nayak S. Influence of different treated cellulose fibers on the mechanical and thermal properties of poly(lactic acid). ACS Sustain Chem & Eng 2016;4:1616—29.

[36] Qian S, Mao H, Zarei E, Sheng K. Preparation and characterization of maleic anhydride compatibilized poly(lactic acid)/bamboo particles. Biocomposites 2015;23:341—7.

[37] Jiang F, Hsieh YL. Chemically and mechanically isolated nanocellulose and their self-assembled structures. Carbohydrate Polym 2013;95:32—40.

[38] Sonia A, Priya Dasan K. Chemical, morphology and thermal evaluation of cellulose microfibers obtained from Hibiscus sabdariffa. Carbohydrate Polym 2013;92:668—74.

[39] Dong Y, Ghataura A, Takagi H, Haroosh H, Nakagaito A, Lau K. Polylactic acid (PLA) biocomposites reinforced with coir fibres: evaluation of mechanical performance and multifunctional properties. Composites: Part A 2014;63:76—84.

[40] Zhu R, Liu H, Zhang J. Compatibilizing effects of maleated poly(lactic acid) (PLA) on properties of PLA/soy protein composites. Indus & Eng Chem Res 2012;51: 7786—92.

[41] Ahmad E, Luyt A. Morphology, thermal, and dynamic mechanical properties of poly(lactic acid)/sisal whisker nanocomposites. Polymer Composites 2012;33:1025—32.

[42] Song Y, Tashiro K, Xu D, Liu J, Bin Y. Crystallization behavior of poly(lactic acid)/microfibrillated cellulose composite. Polymer 2013;54:3417—25.

[43] Fu W. Mechanical and biodegradable properties of L-lactide-grafted sisal fiber reinforced polylactide composites. J Reinforced Plastics and Composites 2014;33:2034—45.

[44] Faludi G, Hári J, Renner K, Móczó J, Pukánszky B. Fiber association and network formation in PLA/lignocellulosic fiber composites. Composites Sc Technol 2013;77:67—73.

[45] Huang L, Zhang X, Xu M, Chen J, Shi Y, Huang C, et al. Preparation and mechanical properties of modified nanocellulose/PLA composites from cassava residue. AIP Adv 2018;8:025116.

[46] Mathew A, Oksman K, Sain M. Mechanical properties of biodegradable composites from poly lactic acid (PLA) and microcrystalline cellulose (MCC). J Appl Polym Sci 2005;97:2014—25.

[47] Zhou L, He H, Li M, Huang S, Mei C, Wu Q. Enhancing mechanical properties of poly(lactic acid) through its in-situ crosslinking with maleic anhydride-modified cellulose nanocrystals from cottonseed hulls. Industrial Crops and Products 2018;112:449—59.

[48] Mofokeng J, Luyt A, Tábi T, Kovacs J. Comparison of injection moulded, natural fibre reinforced composites with PP and PLA as matrices. J Thermoplastic Composite Mater 2012;25:927—48.